ROUTING AND ACTION

MEMORANDUM

ROUTING

TO:(1) Materials Science Division (Varanasi, Chakrapani)

Report is available for review

(2) Proposal Files Report No.: Proposal Number: 62297-MS.20

DESCRIPTION OF MATERIAL

CONTRACT OR GRANT NUMBER: W911NF-12-1-0596

INSTITUTION: University of Manchester

PRINCIPAL INVESTIGATOR: Konstantin Novoselov

TYPE REPORT: Final Report

DATE RECEIVED: 10/18/16 9:57AM

PERIOD COVERED: 1/1/13 12:00AM through 12/31/15 12:00AM

TITLE: Superstructures based on 2D crystals

ACTION TAKEN BY DIVISION

(x) Report has been reviewed for technical sufficiency and IS [x] IS NOT [ ] satisfactory.

(x) Material has been given an OPSEC review and it has been determined to be non sensitive and, except for manuscripts and progress reports, suitable for public release.

(x) Perfomance of the research effort was accomplished in a satisfactory manner and all other technical requirements have been fulfilled.

(x) Based upon my knowledge of the research project, I agree with the patent information disclosed.

Approved by SSL\PANI.VARANASI on 2/15/17 12:38PM

ARO FORM 36-E

REPORT DOCUMENTATION PAGE

Form Approved OMB NO. 0704-0188

1. REPORT DATE (DD-MM-YYYY)	2. REPORT TYPE	3. DATES COVERED (From - To)
18-10-2016	Final Report	1-Jan-2013 - 31-Dec-2015

4. TITLE AND SUBTITLE
Superstructures based on 2D crystals

5a. CONTRACT NUMBER
W911NF-12-1-0596

5b. GRANT NUMBER

5c. PROGRAM ELEMENT NUMBER
611102

6. AUTHORS
Kostya Novoselov, Cinzia Casiraghi

5d. PROJECT NUMBER

5e. TASK NUMBER

5f. WORK UNIT NUMBER

7. PERFORMING ORGANIZATION NAMES AND ADDRESSES
University of Manchester
Oxford Road
-

8. PERFORMING ORGANIZATION REPORT NUMBER

9. SPONSORING/MONITORING AGENCY NAME(S) AND ADDRESS (ES)
U.S. Army Research Office
P.O. Box 12211
Research Triangle Park, NC 27709-2211

10. SPONSOR/MONITOR'S ACRONYM(S)
ARO

11. SPONSOR/MONITOR'S REPORT NUMBER(S)
62297-MS.20

12. DISTRIBUTION AVAILIBILITY STATEMENT
Approved for Public Release; Distribution Unlimited

13. SUPPLEMENTARY NOTES
The views, opinions and/or findings contained in this report are those of the author(s) and should not contrued as an official Department of the Army position, policy or decision, unless so designated by other documentation.

14. ABSTRACT
All applications are limited by the properties of the materials that are available to us. Here we propose a new paradigm in material science: superstructures made by 2-dimensional (2D) crystals.

Single-layer crystals (such as graphene, monolayers of boron nitride, molybdenum disulphide, etc) have a number of exciting properties, often unique and very different from those of their bulk counterparts. However, it is the combinations of these crystals to form 2D heterostructures that promise really endless possibilities. One can create

15. SUBJECT TERMS
graphene, 2D materials, heterostructures, devices, inks, superlattice, ohotodetectors

16. SECURITY CLASSIFICATION OF:			17. LIMITATION OF ABSTRACT	15. NUMBER OF PAGES	19a. NAME OF RESPONSIBLE PERSON
a. REPORT	b. ABSTRACT	c. THIS PAGE			Konstantin Novoselov
UU	UU	UU	UU		19b. TELEPHONE NUMBER +44-161-2754

Report Title

Superstructures based on 2D crystals

ABSTRACT

All applications are limited by the properties of the materials that are available to us. Here we propose a new paradigm in material science: superstructures made by 2-dimensional (2D) crystals.

Single-layer crystals (such as graphene, monolayers of boron nitride, molybdenum disulphide, etc) have a number of exciting properties, often unique and very different from those of their bulk counterparts. However, it is the combinations of those crystals to form 2D heterostructures that promise really endless possibilities. One can create such Van deer Waals (VdW) heterostructures by placing individual 2D crystals one on top of another. This way, 2D materials with very different properties can be combined into one 3D structure, thus producing novel, multifunctional materials: we can combine conductivity of one 2D crystal, mechanical strength of another, chemical reactivity of the third, while the optical properties would be given by the whole superstructure. By carefully choosing and arranging the individual layers in the stack one can tune the parameters of the heterostructure, creating materials with tailored properties, or “materials on demand”.
In this project several type of heterostructures have been created, either to study fundamental properties of graphene and other 2D materials or to fabricate functional devices.

Enter List of papers submitted or published that acknowledge ARO support from the start of the project to the date of this printing. List the papers, including journal references, in the following categories:

(a) Papers published in peer-reviewed journals (N/A for none)

Received		Paper
10/18/2016	2	H. Yang, L. Britnell, A. P. Rooney, E. Lewis, A. Felten, C. R. Woods, V. Sanchez Romaguera, T. Georgiou, A. Eckmann, Y. J. Kim, S. G. Yeates, S. J. Haigh, A. K. Geim, K. S. Novoselov, and C. Casiraghi. Heterostructures Produced from Nanosheet-Based Inks, Nano Letters, (07 2014): 0. doi: 10.1021/nl501355j
10/18/2016	3	Huafeng Yang, Freddie Withers, Elias Gebremedhn, Edward Lewis, Liam Britnell, Alexandre Felten, Vincenzo Palermo, Sarah Haigh, David Beljonne and Cinzia Casiraghi. Dielectric nanosheets made by liquid-phase exfoliation in water and their use in graphene-based electronics, 2D Materials, (06 2014): 0. doi: 10.1088/2053-1583/1/1/011012
10/18/2016	10	E.E. Vdovin, A. Mishchenko, M.T. Greenaway, M.?J. Zhu, D. Ghazaryan, A. Misra, Y. Cao, S.?V. Morozov, O. Makarovsky, T.?M. Fromhold, A. Patanè, G.?J. Slotman, M.?I. Katsnelson, A.?K. Geim, K.?S. Novoselov, L. Eaves. Phonon-Assisted Resonant Tunneling of Electrons in Graphene–Boron Nitride Transistors, Physical Review Letters, ( ): . doi:
10/18/2016	11	E.E. Vdovin, A. Mishchenko, M.T. Greenaway, M.?J. Zhu, D. Ghazaryan, A. Misra, Y. Cao, S.?V. Morozov, O. Makarovsky, T.?M. Fromhold, A. Patanè, G.?J. Slotman, M.?I. Katsnelson, A.?K. Geim, K.?S. Novoselov, L. Eaves. Phonon-Assisted Resonant Tunneling of Electrons in Graphene–Boron Nitride Transistors, Physical Review Letters, ( ): . doi:
10/18/2016	12	J. R. Wallbank, D. Ghazaryan, A. Misra, Y. Cao, J. S. Tu, B. A. Piot, M. Potemski, S. Pezzini, S. Wiedmann, U. Zeitler, T. L. M. Lane, S. V. Morozov, M. T. Greenaway, L. Eaves, A. K. Geim, V. I. Fal'ko, K. S. Novoselov, A. Mishchenko. Tuning the valley and chiral quantum state of Dirac electrons in van der Waals heterostructures, Science, ( ): 575. doi:
10/18/2016	13	Jin-Cheng Zheng, Liang Zhang, A V Kretinin, S V Morozov, Yi Bo Wang, Tun Wang, Xiaojun Li, Fei Ren, Jingyu Zhang, Ching-Yu Lu, Jia-Cing Chen, Miao Lu, Hui-Qiong Wang, A K Geim, K S Novoselov. High thermal conductivity of hexagonal boron nitride laminates, 2D Materials, ( ): 011004. doi:
10/18/2016	14	S. Chakraborty, O. P. Marshall, T. G. Folland, Y.- J. Kim, A. N. Grigorenko, K. S. Novoselov. Gain modulation by graphene plasmons in aperiodic lattice lasers, Science, ( ): 246. doi:
10/18/2016	15	S. Chakraborty, O. P. Marshall, T. G. Folland, Y.- J. Kim, A. N. Grigorenko, K. S. Novoselov. Gain modulation by graphene plasmons in aperiodic lattice lasers, Science, ( ): 246. doi:
10/18/2016	16	S. Kaur, Y.-J. Kim, H. Milton, D. Mistry, I. M. Syed, J. Bailey, K. S. Novoselov, J. C. Jones, P. B. Morgan, J. Clamp, H. F. Gleeson. Graphene electrodes for adaptive liquid crystal contact lenses, Optics Express, ( ): 8782. doi:
10/18/2016	17	S. Kaur, Y.-J. Kim, H. Milton, D. Mistry, I. M. Syed, J. Bailey, K. S. Novoselov, J. C. Jones, P. B. Morgan, J. Clamp, H. F. Gleeson. Graphene electrodes for adaptive liquid crystal contact lenses, Optics Express, ( ): 8782. doi:

10/18/2016	18	S. Son, C. Holroyd, J. Clough, A. Horn, S. Koehler, and C. Casiraghi. Reactivity of Graphene on Different Substrates Towards Hydrogenation, appl. phys. letters, ( ): . doi:
10/18/2016	19	D. McManus, S. Vranic, F. Withers, V. Sanchez-Romaguera, M. Macucci, H. Yang, R. Sorrentino, K. Parvez, S. Son, G. Iannaccone, K. Kostarelos, G. Fiori, C. Casiraghi. Water-based and Biocompatible 2D Crystal Inks: from Ink Formulation to All- Inkjet Printed Heterostructures, Nature Nanotechnology, ( ): . doi:
10/18/2016	9	C. R. Woods, F. Withers, M. J. Zhu, Y. Cao, G. Yu, A. Kozikov, M. Ben Shalom, S. V. Morozov, M. M. van Wijk, A. Fasolino, M. I. Katsnelson, K. Watanabe, T. Taniguchi, A. K. Geim, A. Mishchenko, K. S. Novoselov. Macroscopic self-reorientation of interacting two-dimensional crystals, Nature Communications, ( ): 10800. doi:
TOTAL:	**13**	

Number of Papers published in peer-reviewed journals:

(b) Papers published in non-peer-reviewed journals (N/A for none)

Received	Paper

TOTAL:

Number of Papers published in non peer-reviewed journals:

(c) Presentations

Number of Presentations: 0.00

Non Peer-Reviewed Conference Proceeding publications (other than abstracts):

Received	Paper

TOTAL:

Number of Non Peer-Reviewed Conference Proceeding publications (other than abstracts):

Peer-Reviewed Conference Proceeding publications (other than abstracts):

Received Paper

TOTAL:

Number of Peer-Reviewed Conference Proceeding publications (other than abstracts):

(d) Manuscripts

Received Paper

TOTAL:

Number of Manuscripts:

Books

Received Book

TOTAL:

Received	Book Chapter

TOTAL:

Patents Submitted

Patents Awarded

Awards

C. Casiraghi: Marlow award (2014)

Graduate Students

NAME	PERCENT_SUPPORTED
FTE Equivalent:	
Total Number:	

Names of Post Doctorates

NAME	PERCENT_SUPPORTED
Seok Son	0.50
Weifeng Zheng	0.08
Sam Magee	0.08
FREDDIE WITHERS	0.18
ARTEM MISHCHENKO	0.16
FTE Equivalent:	**1.00**
Total Number:	**5**

Names of Faculty Supported

NAME	PERCENT_SUPPORTED
FTE Equivalent:	
Total Number:	

Names of Under Graduate students supported

NAME	PERCENT_SUPPORTED

FTE Equivalent:
Total Number:

Student Metrics

This section only applies to graduating undergraduates supported by this agreement in this reporting period

The number of undergraduates funded by this agreement who graduated during this period:	0.00
The number of undergraduates funded by this agreement who graduated during this period with a degree in science, mathematics, engineering, or technology fields:	0.00
The number of undergraduates funded by your agreement who graduated during this period and will continue to pursue a graduate or Ph.D. degree in science, mathematics, engineering, or technology fields:	0.00
Number of graduating undergraduates who achieved a 3.5 GPA to 4.0 (4.0 max scale):	0.00
Number of graduating undergraduates funded by a DoD funded Center of Excellence grant for Education, Research and Engineering:	0.00
The number of undergraduates funded by your agreement who graduated during this period and intend to work for the Department of Defense	0.00
The number of undergraduates funded by your agreement who graduated during this period and will receive scholarships or fellowships for further studies in science, mathematics, engineering or technology fields:	0.00

Names of Personnel receiving masters degrees

NAME

Total Number:

Names of personnel receiving PHDs

NAME

Total Number:

Names of other research staff

NAME	PERCENT_SUPPORTED

FTE Equivalent:
Total Number:

Sub Contractors (DD882)

Inventions (DD882)

Scientific Progress

see attachement

Technology Transfer

Final Report

Period covered: 01/01/2013 – 30/06/2016

INTRODUCTION

All applications are limited by the properties of the materials that are available to us: the band-gap in silicon dictates the voltages used in computers and the Young modulus of steel determines the size of the beams used in building construction. Here we propose a new paradigm in material science: superstructures made by 2-dimensional (2D) crystals.

Single-layer crystals (such as graphene, monolayers of boron nitride, molybdenum disulphide, *etc*) have a number of exciting properties, often unique and very different from those of their bulk counterparts. However, it is the combinations of those crystals to form 2D heterostructures that promise really endless possibilities. One can create such Van deer Waals (VdW) heterostructures by placing individual 2D crystals one on top of another. This way, 2D materials with very different properties can be combined into one 3D structure, thus producing novel, multifunctional materials: we can combine conductivity of one 2D crystal, mechanical strength of another, chemical reactivity of the third, while the optical properties would be given by the whole superstructure. By carefully choosing and arranging the individual layers in the stack one can tune the parameters of the heterostructure, creating materials with tailored properties, or "materials on demand". In this way, part of the functionality (and there might be several functionalities) is brought on the level of the design of the material itself (usually it is done on the level of creating a structure from a given material). As the range of available 2D materials broadens, so the possible functionality of the 2D-based heterostructures will cover larger and larger areas.

In this project several type of heterostructures have been created, either to study fundamental properties of graphene and other 2D materials or to fabricate functional devices. Different types of 2D crystals have been used, from single and few-layers made by micro-mechanical exfoliation to liquid-phase exfoliated 2D-materials, which are more suitable for industrial applications. In some cases graphene grown by Chemical Vapour Deposition (CVD) has been included in the heterostructure.

SUMMARY OF THE RESULTS

i) Heterostructures made with micro-chemically exfoliated flakes

We first investigated the best materials to create heterostructures, i.e. those giving sharp and smooth interfaces. While contamination (*ie* hydrocarbons trapped between the crystals) can never been completely removed [1], we observed that substrates such as hexagonal-Boron Nitride (hBN) or Transition Metal Dichalcogenides (TMDCs) are able of "self cleaning": surface contamination assembles into large pockets allowing the rest of the interface to become atomically clean [1]. Devices made by selecting area of the sample that are "bubbles-free" show very high mobilities (20000-500000 $cm^2/V{\cdot}s$). This is fingerprint of the high quality of the interface between the two crystals. However, not all the substrates have the ability of self cleaning: for example images taken by electron microscopy of graphene deposited on atomically

smooth surfaces such as mica, BSCOO, etc show that the contamination is uniformly distributed over all the sample, giving devices with very poor performance (mobility below 1000 $cm^2/V{\cdot}s$).

We further investigate the quality of VdW heterostructures by Raman spectroscopy [2]. Currently, the only method able to provide information about the interface is cross-sectional high-resolution transmission electron microscopy. However, this method is time-consuming and destructive. Therefore, it is essential to develop a fast, simple, and non-destructive technique that can be easily implemented into the device fabrication processes. We have shown that Raman spectroscopy can be used as a non-destructive and rapid technique for probing the VdW forces acting between two atomically thin crystals, where one is a TMDC. In particular, we studied a variety of heterostructures containing MoS_2 monolayer, which is used as a probe to extract information about the interface; graphene, WS_2, and mica acted as the other component of the heterostructure. The Raman spectrum of MoS_2 shows two main Raman-active modes, E_{2g}^1 and A_{1g}. The E_{2g}^1 mode represents an in-plane vibration, and the A_{1g} mode corresponds to an out-of-plane lattice expansion. The A_{1g} strongly depends on the interaction with its neighboring material: for example its position changes with the thickness of few-layers MoS_2. Therefore, we used this Raman mode to extract information on the strength of the vdW interaction between the two adjacent layers. We observed that when the contact between graphene and single-layer MoS_2 is perfect, the A_{1g} position of the heterostructure corresponds to the position of 2-layers MoS_2. The position does not change for increasing number of graphene layers, indicating that the shift is produced only by the interfacial contact between graphene and MoS_2. However, when mica is used instead of graphene, the A_{1g} position is not uniform, indicating that the interface is not perfect over the contact area. It is also noted that the blue shift of A_{1g} on mica is smaller than that shift observed in graphene/MoS_2 heterostructures. This indicates that the interfacial contact is not as good as in the graphene heterostructures, in agreement with transport results [1].

Following optimization of the fabrication process, we then demonstrated functional devices. In previous works, we already demonstrated tunneling transistors and photodetector VdW heterostructures [3-5]. Here we took the complexity and functionality of van der Waals heterostructures to the next level by introducing quantum wells (QWs) engineered with one atomic plane precision. We demonstrated light emitting diodes (LEDs) made by stacking up metallic graphene, insulating hBN and various semiconducting monolayers into complex but carefully designed sequences. Our devices exhibit extrinsic quantum efficiency of nearly 10% and the emission can be tuned over a wide range of frequencies by appropriately choosing and combining 2D semiconductors (monolayers of TMDCs) [6].
Until now, electroluminescence (EL) in TMDC devices has been reported only for lateral monolayer devices and attributed to thermally assisted processes arising from impact ionization across a Schottky barrier and formation of p-n junctions. The use of vertical heterostructures allows us to improve the performance of LED in many respects: reduced contact resistance, higher current densities allowing brighter LEDs, luminescence from the whole device area and wider choice of TMDC and their combinations allowed in designing such heterostructures. The same technology can be extended to create other QW-based devices such as indirect excitonic devices, LEDs based on several different QWs and lasers. Furthermore, we demonstrated that this technology is compatible with flexible substrates: the devices are stable under 1% uniaxial strain.

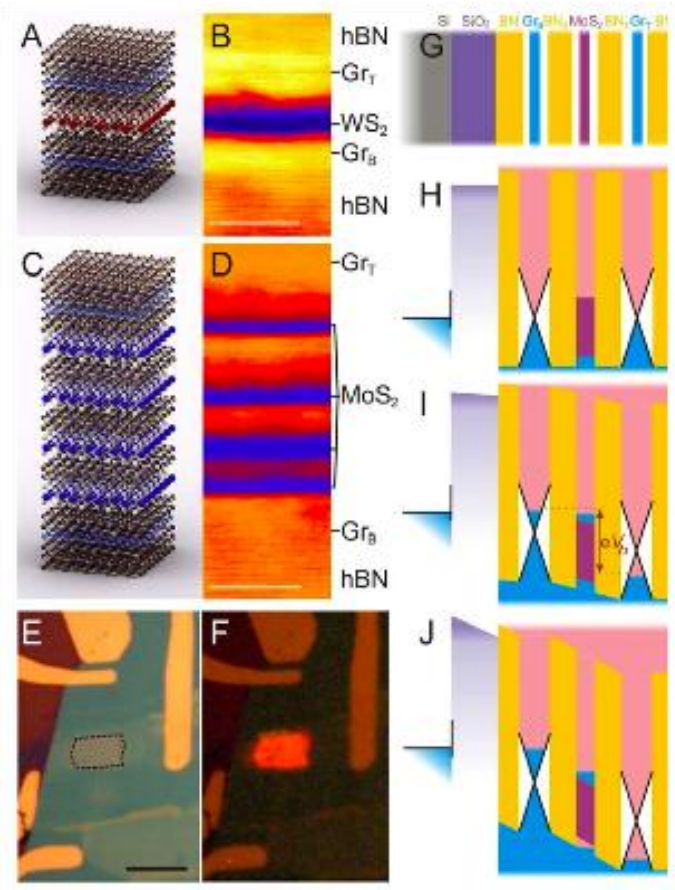

Fig. 1. Heterostructure devices with SQW and MQW. (A) Schematics of SQW heterostructure BN/GrB/2hBN/WS2/2hBN/GrT/hBN. (B) Cross-sectional bright field STEM image of the type of heterostructures presented in (A). Scale bar 5nm. (C, D) Schematics and STEM imaging of hBN/GrB/2hBN/MoS2/2hBN/MoS2/2hBN/MoS2/2hBN/MoS2/2hBN/GrT/hBN. Scale bar 5nm. (E) Optical image of an operational device (hBN/GrB/3hBN/MoS2/3hBN/GrT/hBN). The dashed curve outlines the heterostructure area. Scale bar 10μm. (F) Optical image of EL from the same device. V_b=2.5V, T=300K. (G) Schematic of heterostructure consisting of Si/SiO_2/hBN/GrB/3hBN/MoS_2/3hBN/GrT/hBN. (H-J) Band diagrams for the case of zero applied bias (H), intermediate applied bias (I) and high bias (J) for the heterostructure presented in (G).

Figure 1 schematically shows the architecture of single quantum well (SQW) and multiple quantum well (MQW) structures along with optical and STEM images of a typical device. As active layers we used single and multiple layers of TMDC flakes of MoS_2, WS_2 and WSe_2.
Figure 2 shows the current-voltage (I-V_b) characteristics, photoluminescence (PL) and EL spectra from symmetric devices based on MoS_2. At low V_b, the PL in Fig. 2A is dominated by the neutral A exciton, X_0 peak at 1.93 eV, while the two weaker and broader peaks at 1.87 and 1.79 eV are attributed to bound excitons. At certain V_b, the PL spectrum changes abruptly with another peak emerging at 1.90 eV. This transition is correlated with an increase in the differential conductivity (Fig. 2A) and it is expected to be caused by the increase in the Fermi level in the bottom graphene, which rises above the conduction band in MoS_2, allowing injection of electrons into the QW. In contrast to PL, EL appears only at V_b above a certain threshold, Figs. 2B. We associate such behavior with the Fermi level of top graphene being brought below the

edge of the valence band so that holes can be injected to MoS_2 from the top graphene (in addition to electrons already injected from the bottom graphene), as sketched in Fig. 1J. This creates conditions for exciton formation inside the QW and their radiative recombination. We find that the EL frequency is close to that of PL at $V_b \approx 2.4V$ (Figs. 2A-C), which allows us to attribute the EL to radiative recombination of X-. The quantum emission QE (defined as 2Ne/I, where e is the electron charge, N is the number of the emitted photons and I is the current) is ~ 1%, which is ten times larger than that of planar p-n diodes and 100 time larger than EL from Schottky barrier devices.

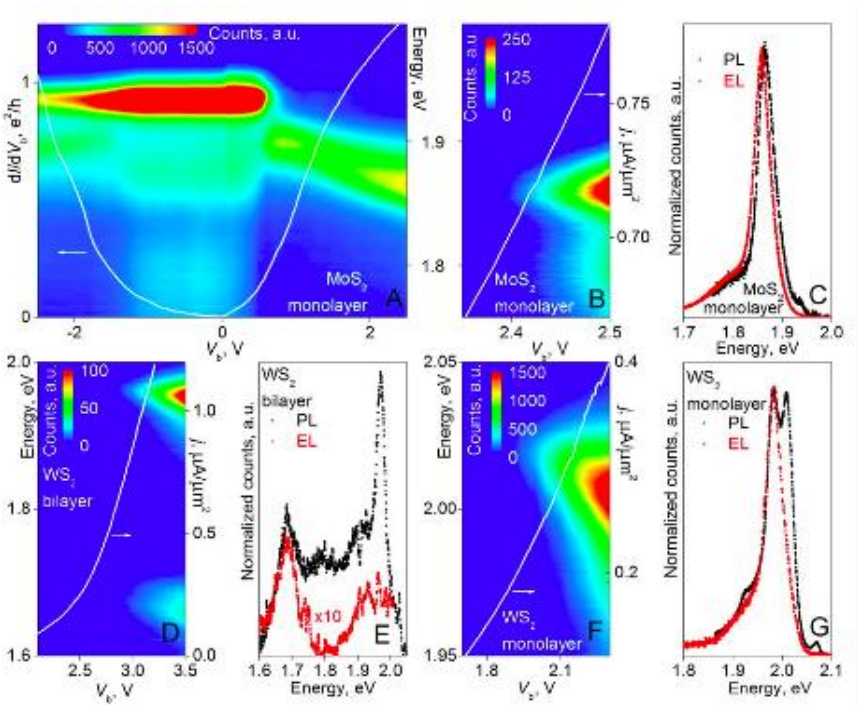

Fig. 2. Optical and transport characterisation of SQW devices, T=7K. (A) Colour map of the PL spectra as a function of V_b for a MoS_2 –based SQW. The white curve is the device's dI/dVb. Excitation energy is 2.33eV. (B) EL spectra as a function of Vb for the same device as in (A). White curve: its j-V_b characteristics (j is the current density). (C) Comparison of the PL and EL spectra for the same device. As PL and EL occur in the same spectral range, we measured them separately. (D,E) and (F,G) Same as (B,C) but for the bilayer and monolayer WS_2 QWs, respectively. The PL curves were taken at V_b=2.4V (C), 2.5V (E) and 2V (G); EL – at V_b =2.5V (C), 2.5V (E) and 2.3V (G).

We have demonstrated that the QE can be further increased by using MQWs stacked in series, which increases the overall thickness of the tunnel barrier and enhances the probability for injected carriers to recombine radiatively.

This technology also offers the possibility of combining various semiconductor QWs in one device. For example we demonstrated a LED made from WSe_2 and MoS_2 QWs, with the following sequence: Si/SiO_2/hBN/GrB/3hBN/WS_2 /3hBN/MoS_2/3hBN/GrT/hB. In comparison with SQW devices, this type of device exhibits more than an order of magnitude stronger both PL and EL, and ~ 5% QE. We associate this with charge transfer between the MoS_2 and WSe_2 layers such that electron-hole pairs are created in both layers but transfer to and recombine in the material with the smaller band-gap. Such a process is expected to depend strongly on band alignment, which is controlled by bias and gate voltages, giving a complex, asymmetric V_b dependence of PL and EL in this device.

Furthermore, we used a heterostructure composed by graphene and hBN to study the effect of a superlattice on the properties of graphene [7]. When a crystal is subjected to a periodic potential,

under certain circumstances (such as when the period of the potential is close to the crystal periodicity; the potential is strong enough, etc.) it might adjust itself to follow the periodicity of the potential, resulting in a, so called, commensurate state. Such commensurate-incommensurate transitions are ubiquitous phenomena in many areas of condensed matter physics: from magnetism and dislocations in crystals, to vortices in superconductors, and atomic layers adsorbed on a crystalline surface. We observed a commensurate-incommensurate transition for graphene on top of hBN. Depending on the rotational angle between the two hexagonal lattices, graphene can either stretch to adjust to a slightly different hBN periodicity (the commensurate state found for small rotational angles) or exhibit little adjustment (the incommensurate state). In the commensurate state, areas with matching lattice constants are separated by domain walls of ~ 2 nm size, where the strain accumulates [7]. This effect might explain recent observations about changes in the electronic, optical, Raman and other properties of graphene-hBN heterostructures. In a more recent work [8], we demonstrated that even the weak interaction which exist between the Graphene and hBN is enough to rotate graphene mechanically by a few degrees, which might be used to create nanomotors operating on atom scale.

Finally, we studied tunnelling phenomena in Gr/hBN/Gr heterostructures. In case of the crystallographic lattices of the two graphene electrodes being almost aligned, the tunnelling current between the graphene layers is determined by the elastic processes, where both energy and the momentum of the electrons are conserved. The J-V_b curve shows a strong peak, followed by a region of negative differential conductance (NDC) [9]. We attribute this peak to resonant tunnelling of carriers between the two graphene electrodes (with momentum conservation). The resonant conditions are demostrated in Fig. 3d, since the tunnelling current is maximized when the momentum difference is compensated by changing electrostatically the energy of the two Dirac cones by an amount $\pm\hbar v_F \Delta K$ (valid only for small mismatch angle). If the bias voltage is too high, the in-plane momentum is conserved only for a small number of states, thus, leading to the reduction in the current. We also performed measurements under magnetic field, applied parallel to the graphene layers, i.e. perpendicular to the tunnel current. One expects the electron to acquire an additional in-plane momentum due to the action of the Lorentz force, which will modify the resonance. This was experimentally confirmed as the bias positions of the resonances are strongly shifted by the in-plane field. Finally, we demonstrated that the resonant tunneling device, due to its resonance peak and negative differential conductance characteristics, induces a tuneable radio-frequency oscillatory current which has potential for future high frequency technology.

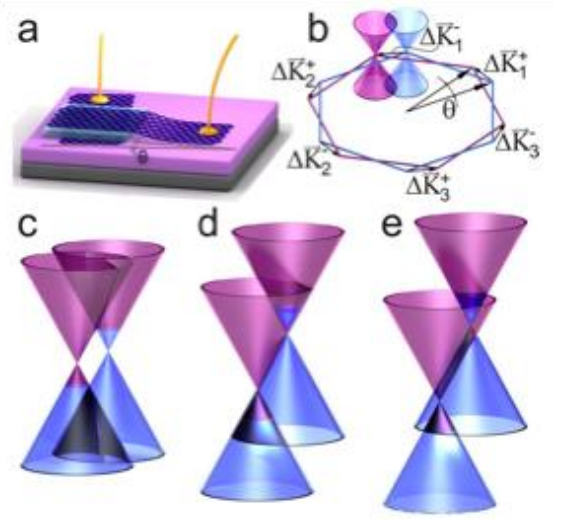

Fig. 3 a) Device schematics: two graphene layers (separated by a BN tunnel barrier shown in light blue); b) A rotation by θ of the two graphene layers in real space corresponds to the momentum shift $\Delta \boldsymbol{K}_{\pm}$ *between two Dirac points. Diagrams c-e represent the relative alignment between top (left cones) and bottom (right cones) graphene Dirac points, for different bias conditions.*

In case of the two graphene electrodes being misoriented, the momentum conservation is satisfied by the phonon emission. Thus, this system presents a very convenient tool to study the phonon spectra of graphene, hBN and their interfaces [10].
In a recent work [11] we demonstrated that the tunnelling current is controlled not only by momentum and energy conservation, but also by pseudospin. Electrons in graphene are described by a vector, two-component, wave-function. Furthermore, they are chiral, which means that there is a very specific relation between the components of the wave-function and the momentum of the electrons. When electrons are tunnelling from one graphene layer to another the interference between the two components of the wave-function results in the effect that only electrons with particular momentum can participate in tunnelling. We can control the selection of the electrons with a particular momentum with the use of in-plane magnetic field – which also allows us to select electrons with particular pseudospin. Thus, we have got a tool that allows injection of electrons in a particular quantum and chiral state.

ii) Heterostructures made with chemically exfoliated flakes

Unfortunately micro-mechanical exfoliation is not suitable for commercial exploitation of graphene-based devices, as this fabrication technique is time consuming, expensive and not mass scalable. Therefore, we also investigated the use of chemically exfoliated 2D crystals for fabrication of heterostructure-based devices. Our approach is based on the use of liquid-phase exfoliation (LPE) to produce dispersions of various 2D crystals. One can then use such inks to deposit platelet layers of different materials sequentially by standard low-cost fabrication techniques (drop- and spray-coatings, inkjet printing, etc.), Figure 4. One of the most important advantages of LPE is that the same method can be used to create inks made of nanosheets of

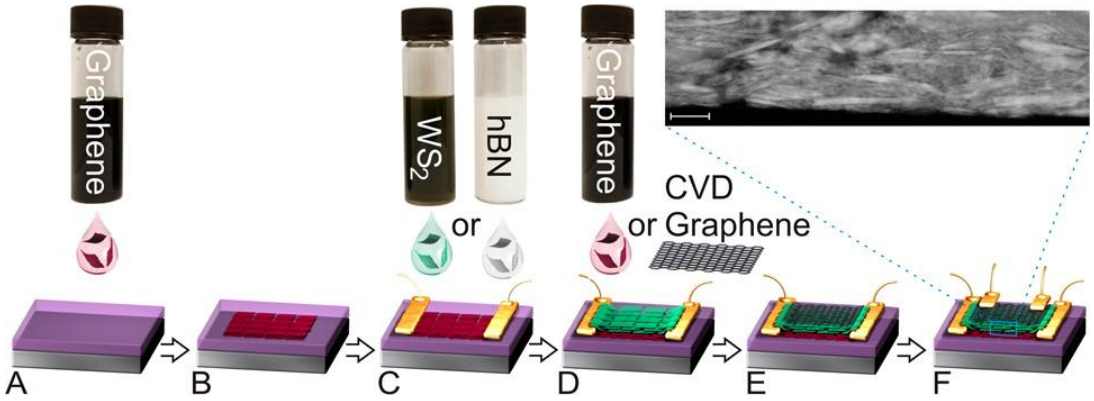

Figure 4 Schematic of a general heterostructure device fabrication process made by using 2D-crystal inks. Last panel shows the final device and the cross-sectional STEM HAADF image of the WS_2 thin film. The scale bar is 35 nm.

different 2D crystals, covering a large variety of properties. Furthermore, this technique is compatible with low-cost and flexible substrates, so it can be combined with flexible electronics.
We used different types of inks, from traditional inks based on organic solvents such as NMP, to water-based inks. The aqueous dispersions have been developed in the framework of another project (GOSPEL, funded by the European Science Foundation). The method is based on the idea of using small poly-aromatic molecules to exfoliate graphite in water and stabilize the dispersion [12]. Our approach has been used to produce inks of graphene, hBN and TMDCs (MoS_2, WS_2, $MoSe_2$ and $MoTe_2$) [13]. In particular hBN inks have relatively high concentration

and are composed by several single-layers, while TMDCs inks are mostly composed by 3-6 layers. We have shown that the 2D crystals nanosheets are defects-free and are compatible with graphene-based devices. In particular, we used LPE hBN as gating dielectric in a planar graphene-based photodetector [13].

We fabricated and tested different types of devices with the following general structure: BGr/barrier/TGr, where TGr and BGr refer to top and bottom graphene electrodes, respectively (Figure 4). We demonstrated that such devices can act as [14]: (i) tunnelling transistors, where tunnelling between TGr and BGr through a barrier (typically made of TMDC) is controlled by a back gate; (ii) photovoltaic devices, where light absorbed in the barrier (TMDC) is converted into photocurrent through TGr and BGr; (iii) in-plane transistors, where TGr is used as a gate and the barrier as a gate dielectric to control the in-plane current in BGr.
The films were deposited by drop-casting and vacuum filtration and they were characterized by Atomic Force Microscopy, Electron Microscopy, Raman spectroscopy and X-Ray Photoelectron Spectroscopy. We did not observe strong changes in the structural properties of the film with the fabrication method. In order to avoid the shortcut between the two electrodes, it is essential to use a pin-hole free barrier in vertical heterostructures: we did observe that filtration is a perfect technique to obtain pin-holes free TMDC films. By placing the membrane in water, we observed that only the first 20 nm of the membrane get removed and floats in the water. By repeating the fishing process several times, ie by depositing these 20 layers one on top of each other, one can strongly minimize the pin-holes density. We observed that already after 2 depositions (*ie* using a TMDC film with a total thickness of ~40 nm), the pin-holes are almost completely eliminated. Therefore, our devices are characterized by TMDCs film of 40-60 nm thickness, which are pin-hole free.
The tunnelling transistors with structure: $Si/SiO_2/BGr/WS_2/TGr$ are characterized by current-bias voltage ($I–V_b$) characteristics which are strongly nonlinear - fingerprint of those type of devices. However, the device shows characteristics very different from the one obtained by micro-mechanical exfoliation [3]. For example the zero-bias conductivity decreases dramatically with decreasing temperature. Such a strong temperature dependence suggests an excitation mechanism for charge carrier generation, either from the graphene electrodes (in this case the tunnelling barrier is the Schottky barrier between graphene and WS_2) or from the impurity band in WS_2 (a strong impurity band is expected due to the large fraction of edges in our nanocrystals of WS_2).
The same device, used as photovoltaic, shows a linear I-V curve under illumination, which demonstrates that in this regime the current is dominated by the photo-excited carriers. Also, finite photocurrent has been observed even at zero bias voltage, demonstrating that such structures can be indeed used as photovoltaic devices. The device is also sensitive to the gate voltage, although again we find that the overall behaviour of the device is very different from the one reported for the same device produced by micro-mechanically exfoliated flakes [5]. We achieved photoresponsivity values of 0.1 mA/W. We also fabricated the same device on plastic and investigate the photo-current stability under bending conditions: the device is stable at least up to 1.5% strain, making this technology compatible with flexible electronics.

In addition we have tested some of the properties of LPE hBN: first, we looked at its dielectric properties [13-14]. Its excellent chemical, mechanical and thermal properties make h-BN thin films a promising dielectric alternative in the next generation of nanodevices. We tested

Si/SiO_2/BGr/hBN/Au devices, where LPE hBN (prepared through filtering of a hBN suspension, with subsequent transfer of the hBN paper from the filter to the device) served as transparent dielectric between the channel (BGr, CVD graphene) and the gate (Au). From the resistivity of the BGr channel as a function of top gate voltage we can estimate the effective dielectric constant of LPE hBN, which is ~ 1.5. The significant deviation from the bulk value (4, as established in recent tunnelling experiments) is due to lose packing of hBN laminates. This low value of the dielectric constant of the LPE hBN could be an advantageous property when considering its incorporation in densely packed electronic elements, where loss needs to be kept to a minimum. Knowing the capacitance to the top gate allows us to estimate the mobility of the BGr to be of the order of 3×10^3 $cm^2/V \cdot s$, which is typical of CVD graphene. This clearly indicates that deposition of LPE hBN does not deteriorate the properties of graphene. Finally, we have also tested the breakdown voltage for our LPE h-BN, which turned out to be 0.25 V/nm [14]. This is comparable (or better) than traditionally used inkjet printed dielectric or the dielectric strength of spattered films. This demonstrates that LPE h-BN can be used as a dielectric for transparent, flexible transistor applications. More recently, we have looked also at its thermal properties, we found that hBN laminates have high thermal conductivity of around 30 W/mK, which is very significant for insulating materials [15].

Finally, in the framework of another project, we have carefully engineered our 2D-crystal formulations to be compatible also with ink-jet printing - a simple, versatile, and low-cost technique for large-scale manufacturing of functional devices.
Available inkjet printable formulations, produced by LPE, are still far from ideal as they are either based on toxic and expensive solvents, or require time-consuming and expensive formulation processing, substrate functionalization or need relatively high temperature to dry, which limits the range of substrates that can be used. In addition, none of those formulations are suitable for thin-films heterostructure fabrication, which requires multi-stack formation with well defined interfaces. Fully printing a multi-layer stack is a very well known challenge in printing technology: the different materials in the stack tend to re-disperse at the interface, producing uncontrolled interfaces, resulting in poor device reproducibility and performance. Better control of interfacial effects and processing conditions allowed significant improvements in the performance of organic field effect transistors. Making new printable formulations of functional materials is very challenging: inkjet printing requires the ink to have specific physical properties; water, for example, is unsuitable for both LPE and inkjet printing. We developed a simple method for production of highly concentrated, stable, inkjet printable, water-based inks that can be formulated for a range of 2D materials [16]. The ink composition has been optimized to achieve optimal film formation for multi-stack formation, allowing fabrication of all-inkjet printed heterostructures, such as arrays of all-printed photosensors over cm^2 areas on plastic and paper and programmable logic devices completely made of 2D-crystals. Devices fully printed on paper show responsivity well above 1 mA/W – several orders of magnitude above typical responsivity found with chemically exfoliated materials. Because the inks are expected to find utility in several applications as different consumer products, we also investigated possible adverse effects from exposure and determined their safety limitations by performing dose-escalation cytotoxicity assays in vitro using lung and skin cells. Overall, no significant cytotoxic responses compared to untreated cells were observed for all doses. Therefore, our inks could find important applications also in drug delivery and biomedical applications.

iii) Other works

1) Graphene can be used as tunable plasmonic material. Here we utilised it in quantum cascade lasers, where graphene tunable plasmonic properties allowed us to discriminate between different lasing modes.

S. Chakraborty, O. P. Marshall, T. G. Folland, Y. J. Kim, A. N. Grigorenko, and K. S. Novoselov, "Gain modulation by graphene plasmons in aperiodic lattice lasers", Science 351(6270), 246-248 (2016).

2) CVD graphene can be used for a number of applications where electrical conductivity and optical transparency are required. In this project we created adaptable contact lenses by creating liquid crystals lenses. The use of graphene is essential here, since no other transparent materials can guarantee conductivity on flexible substrate

S. Kaur, Y. J. Kim, H. Milton, D. Mistry, I. M. Syed, J. Bailey, K. S. Novoselov, J. C. Jones, P. B. Morgan, J. Clamp, and H. F. Gleeson, "Graphene electrodes for adaptive liquid crystal contact lenses", Optics Express 24(8), 8782-8787 (2016).

3) The ability of functionalize graphene with several methods, such as radical reactions, cyclo-additions, hydrogenation and oxidations, allows this material to be used in a large range of applications. In this framework, it is essential to be able to control the efficiency and stability of the functionalization process - this requires understanding how the graphene reactivity is affected by the environment, including the substrate. In this work we provided an insight on the substrate dependence of graphene reactivity towards hydrogenation by comparing three different substrates: silicon, hexagonal boron nitride (h-BN) and molybdenum disulfide (MoS_2). Although MoS_2 and h-BN have flatter surfaces than silicon, we found that the H coverage of graphene on h-BN is about half of the H coverage on graphene on both silicon and MoS_2. Therefore, graphene shows strongly reduced reactivity towards hydrogenation when placed on h-BN.

S. Son, C. Holroyd, J. Clough, A. Horn, S. Koehler, and C. Casiraghi, "Effect of the substrate on hydrogenation and hydrogenation mechanism", Appl. Phys. Lett, under review

4) The hydrogenation mechanism of graphene is not completely understood. From a theoretical point of view, hydrogenation is expected to happen by clustering, i.e. starting from a nucleation point, which corresponds to the formation of the first C-H bond. However, this has never completely verified experimentally. Here we used the roughening dynamic theory to get further insights on the H coverage mechanism.

S. Son, C. Casiraghi, "Insights on the hydrogenation of graphene by using the roughnening dynamics theory", in preparation

5) The superposition of graphene on hexagonal−Boron Nitride (hBN) leads to the creation of a superlattice, which causes a strong reconstruction of the graphene's electronic spectrum with new superlattice Dirac points (SDP) emerging at sub-eV. Changes in the electronic structure are expected to reflect in the Raman spectrum, in particular when shifting the Fermi energy close to

the new Dirac points. In this work we study the Raman spectrum of graphene (Gr) on hBN in both aligned (i.e. Gr/hBN superlattice) and misaligned configurations. We observed strong changes in position and width of G- and 2D-Raman modes in case of gated graphene/hBN superlattices. Those are direct fingerprint of the presence of a period potential distribution.

S. Son, Y. Shin, C. Casiraghi, "Raman spectroscopy of gated graphene/hexagonal-boron nitride superlattices", in preparation

References

1. *Electronic Properties of Graphene Encapsulated with Different Two-Dimensional Atomic Crystals*, A. V. Kretinin, Y. Cao, J. S. Tu, G. L. Yu, R. Jalil, K. S. Novoselov, S. J. Haigh, A. Gholinia, A. Mishchenko, M. Lozada, T. Georgiou, C. R. Woods, F. Withers, P. Blake, G. Eda, A. Wirsig, C. Hucho, K. Watanabe, T. Taniguchi, A. K. Geim, and R. V. Gorbachev, Nano Lett., 2014, 14 (6), pp 3270–3276
2. *Raman Modes of MoS2 Used as Fingerprint of van der Waals Interactions in 2D Crystal-Based Heterostructures*, K-G Zhou, F. Withers,Y. Cao, S. Hu, G. Yu, and C. Casiraghi, ACS Nano, DOI: 10.1021/nn5042703 (2014)
3. *Field-Effect Tunneling Transistor Based on Vertical Graphene Heterostructures*, L. Britnell, et al, Science, 33, 947-950 (2012)
4. *Vertical field-effect transistor based on graphene–WS2 heterostructures for flexible and transparent electronics*, Thanasis Georgiou, Rashid Jalil, Branson D. Belle, Liam Britnell, Roman V. Gorbachev, Sergey V. Morozov, Yong-Jin Kim, Ali Gholinia, Sarah J. Haigh, Oleg Makarovsky, Laurence Eaves, Leonid A. Ponomarenko, Andre K. Geim, Kostya S. Novoselov, Artem Mishchenko, Nature Nanotechnology 8, 100–103 (2013)
5. *Strong Light-Matter Interactions in Heterostructures of Atomically Thin Films*, L. Britnell, R. M. Ribeiro, A. Eckmann, R. Jalil, B. D. Belle, A. Mishchenko, Y.-J. Kim, R. V. Gorbachev, T. Georgiou, S. V. Morozov, A. N. Grigorenko, A. K. Geim, C. Casiraghi, A. H. Castro Neto, K. S. Novoselov, Science, 340, 1311-1314 (2013)
6. *Light-emitting diodes by band-structure engineering in van der Waals heterostructures,* F. Withers, O. Del Pozo-Zamudio, A. Mishchenko, A. P. Rooney, A. Gholinia, K. Watanabe, T. Taniguchi, S. J. Haigh, A. K. Geim, A. I. Tartakovskii & K. S. Novoselov, Nature Materials 14, 301–306 (2015)
7. *Commensurate-incommensurate transition for graphene on hexagonal boron nitride*, CR Woods, L Britnell, A Eckmann, GL Yu, RV Gorbachev, AV Kretinin, et al, Nature Physics 10(6), 451–456 (2014).
8. *Macroscopic self-reorientation of interacting two-dimensional crystals*, C. R. Woods, F. Withers, M. J. Zhu, Y. Cao, G. Yu, A. Kozikov, M. Ben Shalom, S. V. Morozov, M. M. van Wijk, A. Fasolino, M. I. Katsnelson, K. Watanabe, T. Taniguchi, A. K. Geim, A. Mishchenko, and K. S. Novoselov ", Nature Communications 7, 10800 (2016)
9. *Twist-controlled resonant tunnelling in graphene/boron nitride/graphene heterostructures*, A. Mishchenko et al, Nature Nanotechnology 9, 808–813 (2014)
10. *Phonon-assisted resonant tunneling of electrons in graphene-boron nitride transistors*, E. E. Vdovin, A. Mishchenko, M. T. Greenaway, M. J. Zhu, D. Ghazaryan, A. Misra, Y. Cao, S. V. Morozov, O. Makarovsky, T. M. Fromhold, A. Patane, G. J. Slotman, M. I. Katsnelson,

A. K. Geim, K. S. Novoselov, and L. Eaves, Physical Review Letters 116(18), 186603 (2016)

11. *Tuning the valley and chiral quantum state of Dirac electrons in van der Waals heterostructures*, J. R. Wallbank, D. Ghazaryan, A. Misra, Y. Cao, J. S. Tu, B. A. Piot, M. Potemski, S. Pezzini, S. Wiedmann, U. Zeitler, T. L. M. Lane, S. V. Morozov, M. T. Greenaway, L. Eaves, A. K. Geim, V. I. Fal'ko, K. S. Novoselov, and A. Mishchenko, Science (New York, N.Y.) 353(6299), 575-579 (2016).
12. *A simple method for graphene production based on exfoliation of graphite in water using 1-pyrenesulfonic acid sodium salt*, H. Yang, Y. Hernandez, A. Schlierf, A. Felten, A. Eckmann, S. Johal, P. Louette, J-J. Pireaux, X. Feng, K. Mullen , V. Palermo, and C. Casiraghi, Carbon, DOI: 10.1016/j.carbon.2012.11.022 (2012)
13. *Dielectric nanosheets made by liquid-phase exfoliation in water and their use in graphene-based electronics*, Huafeng Yang, Freddie Withers, Elias Gebremedhn, Edward Lewis, Liam Britnell, Alexandre Felten, Vincenzo Palermo, Sarah Haigh, David Beljonne and Cinzia Casiraghi, 2D Mater. 1, 011012 (2014)
14. *Heterostructures Produced from Nanosheet-Based Inks*, F. Withers, H. Yang, L. Britnell, A. P. Rooney, E. Lewis, A. Felten, C. R. Woods, V. Sanchez Romaguera, T. Georgiou, A. Eckmann, Y. J. Kim, S. G. Yeates, S. J. Haigh, A. K. Geim, K. S. Novoselov, and C. Casiraghi, Nano Lett., 2014, 14 (7), pp 3987–3992
15. *High thermal conductivity of hexagonal boron nitride laminates*, J. C. Zheng, L. Zhang, A. V. Kretinin, S. V. Morozov, Y. B. Wang, T. Wang, X. J. Li, F. Ren, J. Y. Zhang, C. Y. Lu, J. C. Chen, M. Lu, H. Q. Wang, A. K. Geim, and K. S. Novoselov, 2D Materials 3(1), 011004 (2016).
16. *Water-based and Biocompatible 2D Crystal Inks: from Ink Formulation to All- Inkjet Printed Heterostructures*, D. McManus, S. Vranic, F. Withers, V. Sanchez-Romaguera, M. Macucci, H. Yang, R. Sorrentino, K. Parvez, S. Son, G. Iannaccone, K. Kostarelos, G. Fiori, C. Casiraghi, Nature Nanotechnology, under review